2D Materials

PAPER

Optical Hall effect in strained graphene

V Hung Nguyen, A Lherbier and J-C Charlier

Institute of Condensed Matter and Nanosciences, Université catholique de Louvain, Chemin des étoiles 8, B-1348 Louvain-la-Neuve, Belgium

E-mail: viet-hung.nguyen@uclouvain.be

RECEIVED
7 December 2016

REVISED
26 January 2017

ACCEPTED FOR PUBLICATION
9 February 2017

PUBLISHED
24 February 2017

Keywords: optical properties, 2D materials, graphene, strain, ab initio, tight binding

Supplementary material for this article is available online

Abstract

When passing an optical medium in the presence of a magnetic field, the polarization of light can be rotated either when reflected at the surface (Kerr effect) or when transmitted through the material (Faraday rotation). This phenomenon is a direct consequence of the optical Hall effect arising from the light-charge carrier interaction in solid state systems subjected to an external magnetic field, in analogy with the conventional Hall effect. The optical Hall effect has been explored in many thin films and also more recently in 2D layered materials. Here, an alternative approach based on strain engineering is proposed to achieve an optical Hall conductivity in graphene without magnetic field. Indeed, strain induces lattice symmetry breaking and hence can result in a finite optical Hall conductivity. First-principles calculations also predict this strain-induced optical Hall effect in other 2D materials. Combining with the possibility of tuning the light energy and polarization, the strain amplitude and direction, and the nature of the optical medium, large ranges of positive and negative optical Hall conductivities are predicted, thus opening the way to use these atomistic thin materials in novel specific opto-electro-mechanical devices.

1. Introduction

The Hall effect [1] is a fascinating phenomenon describing electrical conduction transverse to an applied electric field which is usually obtained thanks to a magnetic field. Its quantized version, the quantum Hall effect, has become one of the key tools for exploring quantum phenomena in 2D mesoscopic systems [2]. Although most of the works have concentrated on static properties, the optical Hall effect (OHE) is another exceptional feature [3]. Indeed, while the longitudinal optical conductivity is related to the light absorption, a finite optical Hall component is the basis of the Faraday rotation and magneto-optic Kerr effect [4]. Studying the OHE, on the one hand, is necessary to understand fully the picture of the dynamics of charges interacting with light and on the other hand, is a guide for magneto-optical applications, e.g. in optical diodes and other non-reciprocal optical elements [5]. Additionally, quantum Hall effect measurements in both DC and AC cases have been known as the basis of metrology applications [6].

In recent years, graphene and 2D layered materials have attracted increasing attention for many fundamental researches and applications [7]. Especially, due to its unusual electrical, optical properties and outstanding mechanical properties, graphene has been shown to be very promising for specific applications in flexible electronics [8], photonics and optoelectronics [9]. In flexible electronics, the attractiveness of graphene lies in its excellent mechanical endurance and high sensitivity of the electronic properties to strain [10]. Due to its unconventional electronic structure with a linear dispersion at low energies, graphene has been widely used for numerous photonic and optoelectronic devices, operating in a broad spectral range from the ultraviolet, visible and near-infrared to the mid-infrared, far-infrared and even to the terahertz and microwave regions [9]. Its applications include transparent electrodes, solar cells, optical modulators and photodetectors [11].

Actually, the optical properties of graphene and related materials have been already reported in numerous published works [12–22]. The OHE in graphene subjected to an external magnetic field has been also theoretically and experimentally explored [23–31]. The magnetic field breaks the time-reversal symmetry in graphene and hence, similarly to the static case, a finite optical Hall conductivity can be achieved. On this basis, the Faraday rotation of a few degrees in modest

magnetic fields has been experimentally observed [24, 26]. It has been also shown that strain engineering is an efficient technique to modulate the optical properties of graphene [32–36]. In particular, the strain can break the lattice symmetry and the optical spectrum of graphene exhibits strong anisotropy and dichroism [32, 33, 36]. These findings appeal for an in-depth investigation of the optical Hall conductivity in strained graphene, which is still missing.

The aim of the present work is to investigate thoroughly the emergence of OHE in graphene systems subjected to strain, using the density functional theory (DFT) and parametrized tight-binding (TB) approaches[1]. It is found that when strain is applied, a finite optical Hall conductivity is observed in graphene even though magnetic field is zero. Especially, this conductivity has rich properties, compared to the longitudinal component and conventional Hall effect obtained under an external magnetic field. In particular, the strain-induced Hall conductivity can be modulated while its sign can be reversed by tuning incident light (frequency and polarization) and/or strain (magnitude and direction). Finally, it is worth noting that this strain-induced OHE is demonstrated to be common for many other 2D materials and the explored properties could be the basis of several novel applications in opto-electro-mechanical systems.

2. Methods

2.1. First-principles calculations

First-principles calculations were performed using the self-consistent density functional theory (DFT) within the GGA–PBE approach implemented in the SIESTA [37] package. The complex optical conductivity tensor σ_{pq} is derived from the complex dielectric tensor ε_{pq} using the formula $\sigma_{pq}(\omega) = -\mathrm{i}\omega\varepsilon_0\varepsilon_{pq}(\omega)$, where ε_0 is the vacuum dielectric constant. Note that the calculation of ε_{pq} requires a specific treatment because of the 2D nature of the system. Further details can be found in the supplementary material.

2.2. Tight-binding calculations

The tight binding (TB) calculations for graphene were performed within a third-nearest-neighbors orthogonal model that has been demonstrated to give reasonably accurate results, compared to the DFT ones [38]. In this work, the parameters (i.e. onsite energy and three hopping terms) of this TB model were elaborated from the DFT data so as to achieve the best agreement between the two methods in the calculation of the electronic bandstructure and the optical conductivities (see supplementary material). The TB optical conductivities are computed using the standard Kubo formula [20, 21]:

$$\sigma_{pq}(\omega) = \frac{2e^2\hbar}{\mathrm{i}S}\sum_{\mathbf{k}\epsilon\mathbf{BZ}}\sum_{n,m}\frac{f(E_n)-f(E_m)}{E_n(\mathbf{k})-E_m(\mathbf{k})} \times \frac{\langle n|\hat{v}_p|m\rangle\langle m|\hat{v}_q|n\rangle}{\hbar\omega + E_n(\mathbf{k}) - E_m(\mathbf{k}) + \mathrm{i}\eta} \quad (1)$$

where S is the area of the primitive cell, $f(E)$ is the Fermi distribution function, $E_{n,m}(\mathbf{k})$ and $|n, m\rangle$ represent the eigenenergies and eigenstates of the system, $\hat{v}_{p/q}$ are the velocity operators, and η is a phenomenological broadening.

When strain is applied, the graphene lattice is deformed and the $C-C$ bond length is hence modified. Taking into account this effect, the TB hopping energies are modified following the exponential decay law as in [39]. The detailed description of this calculation method can be also found in the supplementary material.

3. Results

Both DFT and TB approaches described above were employed to investigate the opto-electro-mechanical graphene systems schematized in figure 1(a) where a linearly polarized light with energy $\hbar\omega$ and polarization angle ϕ is considered and an in-plane uniaxial strain of magnitude ϵ is applied in the direction θ with respect to the armchair direction of graphene.

In figures 1(b) and (c), the optical conductivity components are computed as a function of light energy in monolayer graphene without and with strain. As seen, our parametrized TB calculations reproduce very well the DFT results at low and high energies. A slight discrepancy between two methods occurs only in the medium energy range where the conductivity peaks are present. In spite of this fact, the two methods are still in very good agreement for the investigation of the overall spectrum of optical conductivities in both unstrained and strained graphene systems (see the further demonstration in the supplemental material). Very remarkably, the optical Hall conductivity is found to be zero for unstrained graphene but exhibits finite values when strain is applied. This is accompanied by a peak splitting in the longitudinal optical conductivity spectrum. Throughout the work, the considered systems are undoped. In doped cases, a well-known phenomenon is observed, i.e. the Pauli blocking mechanism comes into play and hence all the optical spectra exhibits a finite gap at low energies (e.g. as seen in [21]).

In order to understand the origins of the optical Hall effect observed, the effects of strain on the optical conductivities are investigated in more detail in figure 2. Note that in the graphene bandstructure, there are six Dirac cones at the corners (K-points) of its Brillouin zone, however, they are characterized by only two distinguishable ones. Accordingly, six saddle (M-) points occur in the middle of these Dirac cones and only three are distinguishable. In the unstrained case, these saddle points are degenerate but can be separated in the energy

[1] See the supplementary material for the detailed description of calculation methodologies and the illustration of Faraday rotation of a circularly polarized light stacks.iop.org/TDM/4/025041/mmedia.

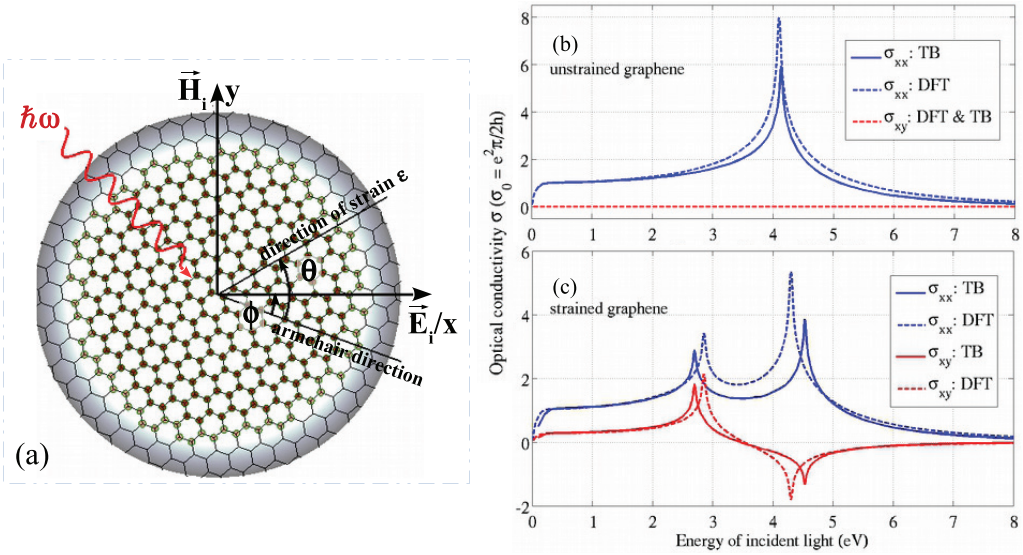

Figure 1. Schematic representation of the opto-electro-mechanical graphene-based system (a). Optical conductivities, predicted by both DFT (dashed) and TB (solid lines) calculations, in graphene without (b) and with strain (c).

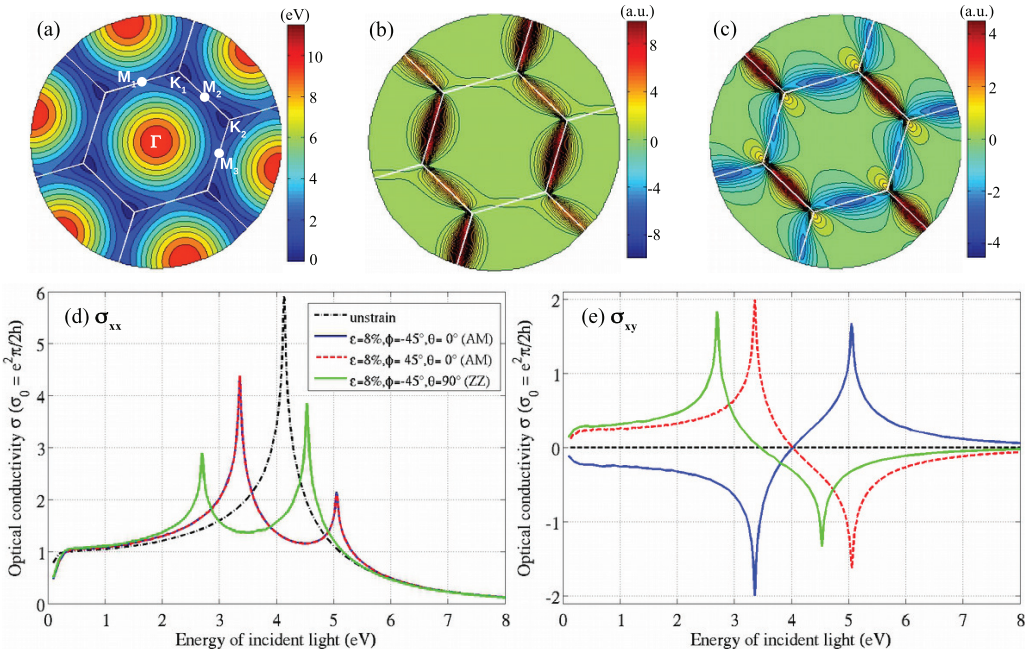

Figure 2. Conduction bands (a), transition coefficients $P_{xx}(\vec{k})$ (b) and $P_{xy}(\vec{k})$ (c) (see text) are presented for light polarization $\phi = -45°$ and uniaxial strain $(\epsilon, \theta) = (8\%, 75°)$. Longitudinal optical conductivity (d) and optical Hall component (e) in uniaxial strained graphene obtained for different ϕ and θ angles.

when strain is applied (see the energy color map in figure 2(a)). Because the optical transitions of charges around the Γ-point are low (see in figures 2(b) and (c) and the related discussions below), the optical spectra of graphene can be basically understood by analyzing the transitions around *K*- and *M*- points. Indeed, the optical transitions around the *K*-points with a linear energy dispersion result in an almost flat spectrum of the longitudinal conductivity σ_{xx} with a universal value of $\sigma_0 = e^2/4\hbar$ at low energies for monolayer graphene [18–21] (see figure 2(d)). At moderately high energies when the transitions around the *M*-points take place, this conductivity exhibits a relatively high peak, which is essentially due to high optical transitions and high density of states of graphene at these points. Note that taking into account the many body effects and other scatterings can lead to corrections to the position of this saddle-point peak and its value. In particular, a position shift of about 10% the saddle-point energy toward high energy should be applied to our calculated optical

spectra, compared to the data in [18]. The peak value is strongly dependent on the effects of all scatterings involved (e.g. see [40]). These effects can be effectively described by introducing properly the broadening factor η in equation (1) however are beyond the scope of the current work. When strain is applied, two main features occur. First, strain effects make graphene lattice very anisotropic, leading to a strong anisotropy of the absorption spectrum, i.e. the conductivity σ_{xx} is strongly dependent on the light polarization and strain direction (see the further details in [32, 33]). Second, as already mentioned, the strain can break the degeneracy of saddle points, leading to the separation of the peaks of σ_{xx} as presented in figures 1(c) and 2(d).

Now, the OHE in strained graphene is explored, i.e. a finite strain-induced conductivity σ_{xy} as displayed in figures 1(c) and 2(e). One of the key terms to determine the conductivity σ_{pq} from the Kubo formula in equation (1), and hence understand the underlying mechanism of this OHE, is the optical transition functions $P_{pq}(\vec{k}) = \langle s_v|\hat{v}_p|s_c\rangle\langle s_c|\hat{v}_q|s_v\rangle$. Here, $|s_{v,c}\rangle$ are eigenstates in the valence/conduction bands, respectively. Different from $P_{xx}(\vec{k})$ that is a non-negative function (see figure 2(b)), $P_{xy}(\vec{k})$ is either positive or negative when considering the whole Brillouin zone of graphene (see in figure 2(c)). The Hall conductivity can be hence rewritten as $\sigma_{xy} = \sigma^{+}_{xy} - \sigma^{-}_{xy}$ where $\sigma^{\pm}_{xy}$ are the absolute values of terms corresponding to positive and negative $P_{xy}(\vec{k})$, respectively. In unstrained case, $\sigma^{+}_{xy} = \sigma^{-}_{xy}$ and hence the conductivity σ_{xy} is totally zero for any polarization and energy of light. In strained graphene, the equality of $\sigma^{\pm}_{xy}$ is broken by strain, leading to a finite σ_{xy}. Physically, it can be understood that in analogy to the magnetic-field effects that break the time-reversal symmetry, the lattice symmetry breaking by strain changes the optical responses and hence results in the OHE in graphene. Note that in this work, we consider uniform strains and hence there is no pseudo magnetic field as observed in graphene under a strain gradient [41].

For all cases presented in figure 2(e), two interesting properties of σ_{xy} are found. First, similarly to the conductivity σ_{xx}, the Hall conductivity σ_{xy} exhibits an almost flat spectrum in the low energy regime and tends to zero at very high energies. In the low energy limit, σ_{xy} can be also estimated by the simple Dirac model as in [36]. Second, high peaks of σ_{xy} are also observed, especially, at the same energies as for the σ_{xx}-component (see figures 1(c) and 2(d), (e)). However, while σ_{xx} is always positive, the full spectrum of σ_{xy} presents both positive and negative peaks and accordingly, two (low and high) energy regimes where this Hall conductivity has opposite signs. This novel property can be understood as follows. As mentioned, $P_{xy}(\vec{k})$ can be either positive or negative in specific areas of the Brillouin zone of graphene. Simultaneously, when strain is applied, the graphene bandstructure is deformed, leading to the separation of degenerate bands in such different areas. Because of these two features, two terms $\sigma^{\pm}_{xy}$ are alternatively dominant in different energy regimes, leading to opposite Hall conductivities at low and high energies as observed. Additionally, this Hall conductivity is also predicted to be strongly anisotropic (see the detailed discussions below), similar to the σ_{xx} component [32, 33].

In the following, the possibilities of achieving and tuning a large Hall conductivity are investigated. First, the Hall conductivity obtained for different uniaxial strains is displayed in figure 3(a) The light polarization $\phi = -45^{\circ}$ is chosen so as to achieve the largest σ_{xy} for strains applied along the direction $\theta = 90^{\circ}$ (see figure 4 below). At low energies, the Hall conductivity is gradually increased when increasing the strain magnitude and, particularly, reaches $\sim 0.5\sigma_0$ for $\epsilon = 10\%$ and $\hbar\omega = 1.5$ eV. At high energies, σ_{xy}-peaks occur and are very rapidly increased for low strains, i.e. they reach values larger than σ_0 for a small strain of only 2%, and progressively saturate at large strains. Basically, the high peaks of $\sigma_{xy} \sim 1 \div 2\sigma_0$ can be achieved for a strain of only a few percents. In order to further enlarge σ_{xy} (e.g. to achieve large Faraday/Kerr rotations), another strategy is suggested [18], i.e. to use few-layer graphene systems. Indeed, as presented in figure 3(b), the Hall conductivity is almost linearly increased as a function of number of graphene layers N_L. In particular, extremely large peaks of σ_{xy}, $\sim 13\sigma_0$ at $\hbar\omega \simeq 2.67$ eV and $\sim -10\sigma_0$ at 4.51 eV, and a large value $\sim 5\sigma_0$ at 2 eV are achieved for a uniaxial strain of 8% and $N_L = 10$.

The effect of shear strains is also investigated in figure 3(c). Interestingly, a smaller shear strain than uniaxial one is required in order to achieve a similarly large σ_{xy}. Our calculations show that overall, the amplitude of Hall conductivity is proportional to the off-diagonal term ϵ_{xy} of the strain tensor (see supplementary material). In the Oxy axis chosen as in figure 1(a), $\epsilon_{xy} = (1+\alpha)\sin(2(\theta-\phi))\epsilon/2$ and $\cos(2(\theta-\phi))\epsilon$ for uniaxial and shear strains, respectively, with the Poisson ratio $\alpha = 0.165$ [42]. On this basis, the largest σ_{xy} is respectively proportional to $(1+\alpha)\epsilon_{\text{uniaxial}}/2$ and ϵ_{shear}, i.e. with two strains satisfying $\epsilon_{\text{shear}}/\epsilon_{\text{uniaxial}} \simeq (1+\alpha)/2 = 0.5825$ the similar σ_{xy}-magnitude can be achieved as shown for $\epsilon_{\text{shear}} = 4\%$ and $\epsilon_{\text{uniaxial}} = 6.8\%$ in figure 3(c).

Achieving both positive and negative values of the Hall conductivity is a very novel/ promising result for practical applications (see the discussions below). As presented in figures 2 and 3, the sign of σ_{xy} can be reversed by tuning the light energy. In figure 3(a), another possibility of reversing this conductivity is also found, i.e. by switching from positive to negative strain.

As already shown in figure 2, the Hall conductivity induced by strain is predicted to be strongly anisotropic, i.e. strongly dependent on the light polarization and strain direction. In figure 4, colormaps showing the full dependence of σ_{xy} on the directions of light polarization and strain are presented. For a given strain (see figures 4(a)–(c), 4(g) and (h)), the ϕ-dependence of σ_{xy} generally satisfies the simple rule

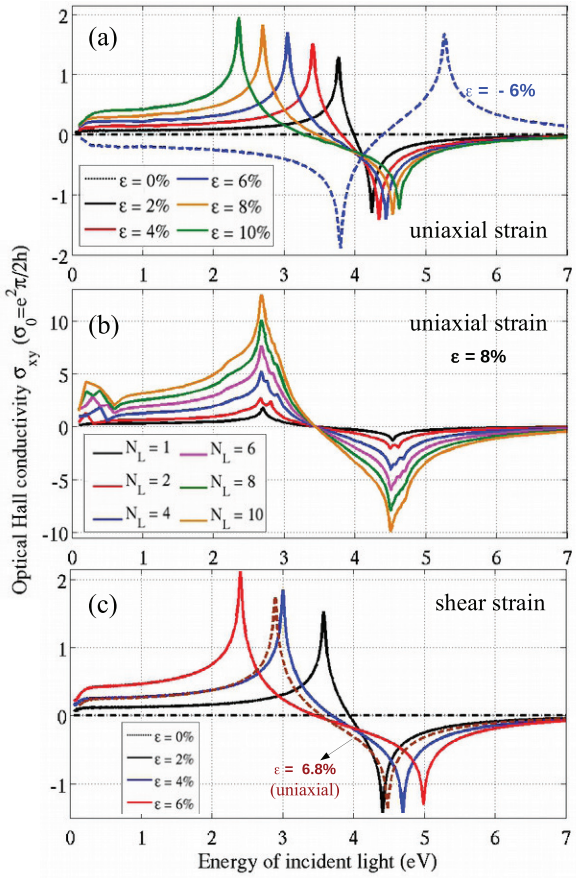

Figure 3. Optical Hall conductivity in monolayer graphene with different strains ((a) and (c)) and in few-layer systems (b). Uniaxial ($\theta = 90°$)/shear ($\theta = 45°$) strains are applied in ((a)–(c)), respectively. The light polarization is fixed to $\phi = -45°$.

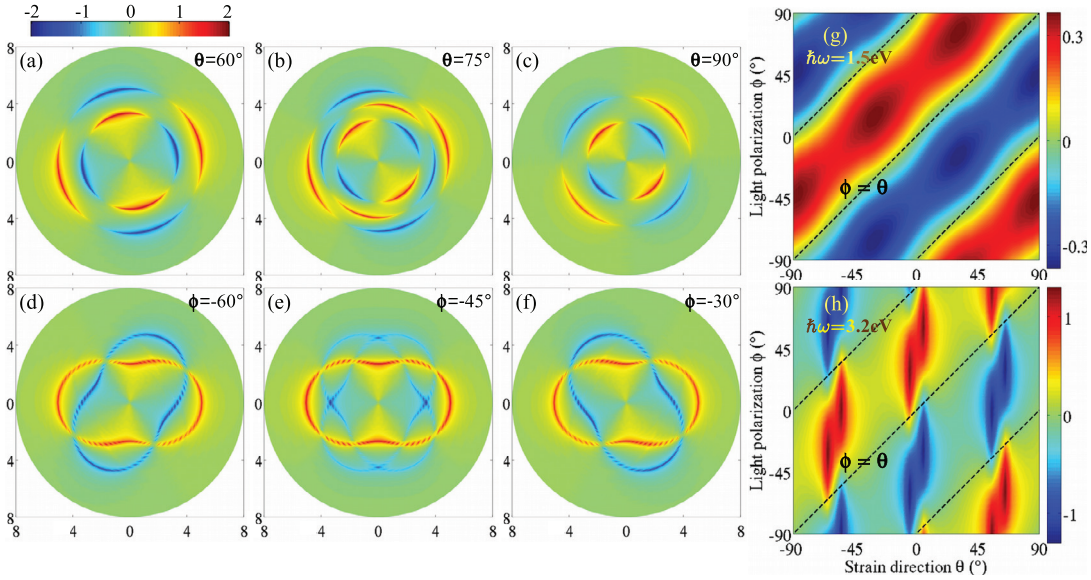

Figure 4. Optical Hall conductivity in monolayer graphene with respect to the light energy $\hbar\omega$ (>0 and in eV) and polarization ϕ, and the strain direction θ. The polar axis of (a)–(f) presents the energy $\hbar\omega$ while the azimuthal direction indicates the angles ϕ in (a)–(c) and θ in (d)–(f). The dashed lines in ((g) and (h)) indicate the cases $\phi - \theta = n\pi/2$. The amplitude of uniaxial strain is fixed to $\epsilon = 8\%$.

$\sigma_{xy} \propto \sin(2(\phi - \theta - \theta_s))$ where θ_s is a function of ω, ϵ and θ. At low energies, θ_s is approximately zero for all strain directions. For a given light polarization (see figures 4(d)–(h)), the θ-dependence of σ_{xy} also satisfies the same rule at low energies but due to the presence of σ_{xy}-peaks, becomes more complex at high energies. Additionally, the peaks of σ_{xy} in (ω, θ)-maps presents three specific peanut lines with the symmetry under a rotation of 60° (see in figures 4(d)–(f)). The full spectrum of σ_{xy} generally presents three peaks but only

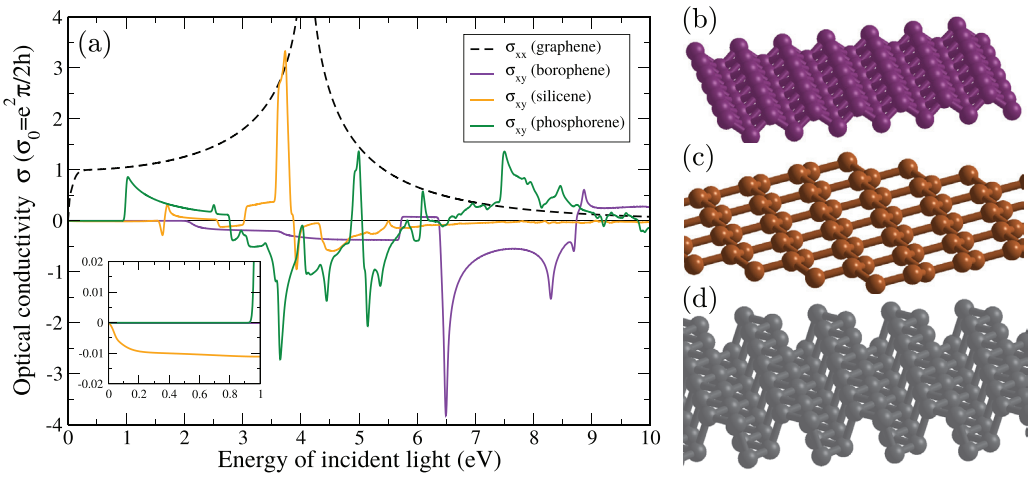

Figure 5. Strain-induced optical Hall effect (a) in borophene (b), silicene (c), and phosphorene (d). A uniaxial strain of 4% is applied in the direction $\theta = 0°$ while the light polarization is $\phi = 45°$. The inset in (a) is a zoom of the optical Hall conductivities at low energies.

two peaks are observed if the light polarization or strain direction is parallel to the armchair or zigzag directions of graphene (see figures 2 and 4(a), (c), (d), (f)). Actually, when uniaxial strain is applied, there are two symmetry directions of lattice deformation, i.e. either parallel or perpendicular to the strain direction. The most common property observed here is that σ_{xy} is generally high if $\phi - \theta \simeq n\pi/2 + \pi/4$ and low if the light polarization is parallel to any symmetry direction of lattice deformation mentioned above, i.e. $\phi - \theta \simeq n\pi/2$ as seen in figures 4(g) and (h). Therefore, the overall dependence of σ_{xy} on ϕ and θ generally satisfies the rule $\sigma_{xy} \propto \sin(2(\phi - \theta))$ although it is considerably disturbed by the presence of σ_{xy}-peaks at high energies (see figure 4(h)). For shear strains, this rule becomes $\sigma_{xy} \propto \cos(2(\phi - \theta))$ as discussed above for figure 3(c). Most interestingly, the direction dependence explored here suggests other possibilities of controlling the sign of σ_{xy}, i.e. by changing the light polarization and strain direction.

Finally, it is worth noting that in analogy to the effect of an external magnetic field, the present opto-electro-mechanical effect is essentially due to the lattice symmetry breaking and hence completely general, i.e. it can be observed in many other 2D materials even though they are metallic, semimetallic or semiconducting. As some examples, *ab initio* optical Hall conductivities calculated in silicene, borophene, and phosphorene are presented in figure 5, which demonstrates that the mechanism explored in this study is indeed very general. Note however, that the optical Hall conductivity remains zero until the optical gap is reached. For instance, while borophene is a metal, optical transitions occur only for energies above 2–3 eV (depending on the applied strain) [43]. For phosphorene, the energy threshold for transitions is ∼1 eV at the level of DFT but the optical gap can be modified because of screening and exitonic effects. Finally, due to its similar bandstructure at low energies, there is no gap for the optical Hall conductivity in silicene (see the inset of figure 5), but its value is much smaller than that obtained in graphene. The latter might be explained by a lower Fermi velocity in silicene compared to graphene as the optical transitions are proportional to the expectation value of velocity operators (see supplementary material).

4. Discussion

First, we would like to give a comparison between this opto-electro-mechanical effect and that induced by an external magnetic field. Essentially, the effects of strain investigated here are different from those of a magnetic field. A magnetic field can break the time-reversal symmetry and result in cyclotron orbits and quantum Landau spectrum while strain simply breaks the lattice symmetry of the system. On this basis, the optical Hall conductivity induced by a magnetic field is a step like function of Fermi energy (due to the quantum Landau spectrum) [23] but it is not the case of strained materials. Additionally, the conductivity induced by a magnetic field in graphene is an oscillating function but decays rapidly when increasing the light energy [23–25]. A very large magnetic field has to be hence applied to achieve a significant value of σ_{xy} in the range of visible light. As demonstrated, the effects of strain seem to be more promising regarding this point. Next, the strain-induced Hall conductivity is strongly directional dependent (i.e. strongly depends on the direction of strain and light polarization) while the conductivity induced by a magnetic field is independent on the light polarization. Finally, the Hall conductivity reported in [23–25] ranges from a few to ten times of the universal value σ_0 for a magnetic field as large as 10 Tesla. This large value of σ_{xy} can be achieved by strain in few layer systems as shown above.

Now, let us discuss other novel properties of this strain-induced OHE and related possible applications.

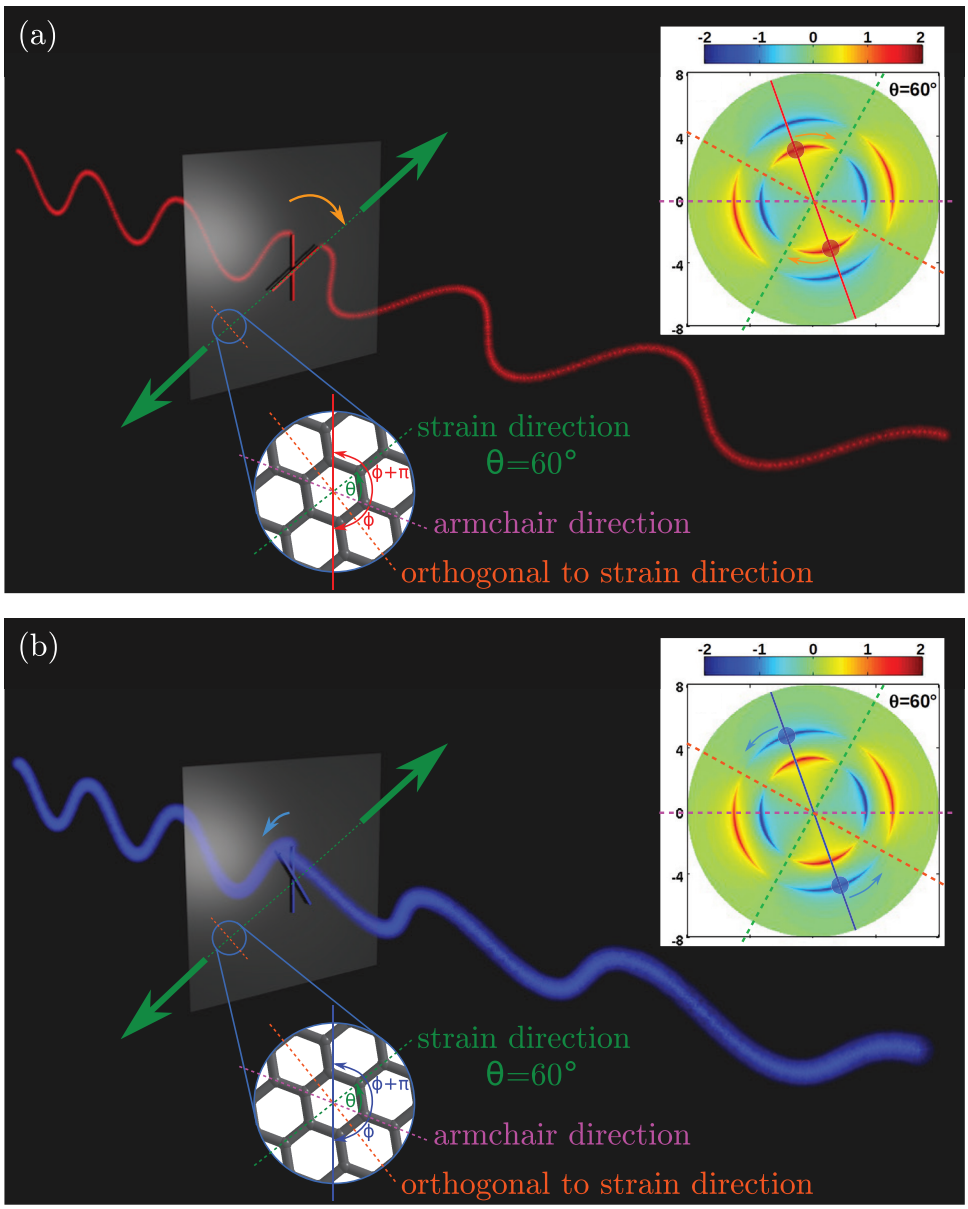

Figure 6. Faraday rotation with low (a) and high (b) energies of the incident light.

First, a finite σ_{xy} can be achieved under zero magnetic field. Second, different from the longitudinal component, the sign of this conductivity can be reversed by tuning the light energy and polarization, changing the strain type (i.e. from positive to negative) and its direction. These switching possibilities can be exploited to explore novel applications in opto-electro-mechanical devices. Third, extremely large σ_{xy} can be observed when shining on the system by a light beam with appropriate energy and can be further enlarged using few-layer systems, of course, at the expense of higher transmittance loss. This is an important ingredient for designing efficient Faraday rotators and related applications.

Interestingly, with the binary property of σ_{xy} when varying the ligh energy and its polarization, the designed Faraday rotator can work as an optical polarizer with a specific output polarization that is dependent on and can be controlled by tuning the strain direction. Indeed, figure 6 illustrates this feature in the case of strain angle $\theta = 60°$. The linearly polarized light carries an electric field oscillating along a given axis determined by the angle ϕ (see in figure 1 and the red line in figure 6(a)). In the low energy regime and for the chosen angle ϕ as in the figure 6(a), the corresponding value of the Hall conductivity is positive (see inset) and therefore the light rotates in the clockwise direction (orange arrow) towards the axis determined by the strain direction (green axis). When its polarization is aligned with the strain direction, σ_{xy} is zero and hence the light does not rotate anymore. It is worth noting that due to the dependence of σ_{xy} (i.e. both intensity and sign) on the light polarization ϕ as presented in figures 4(a)–(c) and more clearly in figure 4(g), all the light beams in the low energy regime are always rotated towards the strain axis either with a clockwise or anti-clockwise rotation. Note that by symmetry, the two directions ϕ and $\phi + 180°$ are equivalent. The direction orthogonal to the strain (dark orange axis) presents also $\sigma_{xy} = 0$ but corresponds to

a saddle point since for any small deviation, the light rotates away from this point. Such a device can thus be used as an efficient light polarizer in the sense that it does not only filter polarized light but also convert light that is not correctly oriented into the desired orientation determined by the direction of applied strain.

Additionally, if one now considers linearly polarized light with several frequencies, it is possible to separate the spectrum into two parts. As discussed above, the low energy components of the incoming light rotate towards the strain axis. In the high energy regime the optical Hall conductivity has a opposite sign, compared to that obtained at low energies. Therefore, as illustrated in figure 6(b), the high energy components rotate towards the axis orthogonal to the strain direction. Thus, the incoming light can be separated into two beams having orthogonal polarizations with the energy threshold (∼3–4 eV depending on the applied strain), which is the energy point where the sign of $\sigma_{xy}(\omega)$ is reversed.

With these properties discussed above, the system can also act as a converter of circularly polarized light into a linearly polarized light. Actually, a circularly polarized light can be considered as a combination of two orthogonal and dephased linearly polarized lights. Since these two linearly polarized lights can be subjected to opposite Faraday rotations, the transmitted light becomes linearly polarized along to the strain (resp. its orthogonal) axis in the case of low (resp. high) energies, respectively, with an amplified electric field (see supplementary material).

Finally, it is worth noting that since the transmittance is extremely high in the considered thin 2D systems [43], the intensity of transmitted light maintains high values compared to the incoming one, which is different from 3D systems where a large part of light can be reflected or absorbed.

5. Conclusion

Strain engineering has been demonstrated to be a novel and alternative approach to efficiently generate optical Hall effect in graphene and 2D materials. Compared to the conventional effect observed under an external magnetic field, the strain-induced optical Hall conductivity exhibits rich properties, i.e. its value can be modulated whereas its sign can be reversed by tuning incident light (frequency and polarization) and/or strain (magnitude and direction). The observed properties could be exploited to explore novel optical devices and, particularly, specific applications in opto-electro-mechanical 2D systems.

Acknowledgments

The authors would like to thank Prof Benoît Hackens (UCL) for fruitful comments and discussions. The work was supported by the FRS–FNRS of Belgium through the research project (N° T.1077.15), by the Fédération Wallonie–Bruxelles through the ARC entitled *3D Nanoarchitecturing of 2D crystals* (N° 16/21-077) and by the European Union's Horizon 2020 research and innovation programme (N° 696656). Computational resources have been provided by the supercomputing facilities of the Université catholique de Louvain (CISM/UCL) and the Consortium des Equipements de Calcul Intensif en Fédération Wallonie Bruxelles (CECI) funded by the FRS–FNRS under the convention N° 2.5020.11.

References

[1] Hall E H 1879 *Am. J. Math.* **2** 287–92
[2] Prange R E and Girvin S M 1990 *The Quantum Hall Effect* 2nd edn (New York: Springer)
[3] Schubert M *et al* 2016 *J. Opt. Soc. Am.* A **33** 1553–68
[4] Kargarian M *et al* 2015 *Sci. Rep.* **5** 12683
[5] Bi L *et al* 2011 *Nat. Photon.* **5** 758–62
[6] Schurr J 2016 *IEEE Trans. Instrum. Meas.* **19** 24–6
[7] Ferrari A C *et al* 2015 *Nanoscale* **7** 4598–810
[8] Jang H *et al* 2016 *Adv. Mater.* **28** 4184–202
[9] Bonaccorso F *et al* 2010 *Nat. Photon.* **4** 611–22
Sun Z *et al* 2016 *Nat. Photon.* **10** 227–38
[10] Si C *et al* 2016 *Nanoscale* **8** 3207–17
[11] Koppens F H L *et al* 2014 *Nat. Nanotechnol.* **9** 780–93
[12] Grüneis A *et al* 2003 *Phys. Rev.* B **67** 165402
[13] Nair R R *et al* 2008 *Science* **320** 1308
[14] Stauber T *et al* 2008 *Phys. Rev.* B **78** 085432
[15] Yang L *et al* 2009 *Phys. Rev. Lett.* **103** 186802
[16] Wright A R *et al* 2009 *Phys. Rev. Lett.* **103** 207401
[17] Yang C H *et al* 2010 *Phys. Rev.* B **82** 205428
[18] Mak K F *et al* 2011 *Phys. Rev. Lett.* **106** 046401
[19] Yuan S *et al* 2011 *Phys. Rev.* B **84** 195418
[20] Moon P and Koshino M 2013 *Phys. Rev.* B **87** 205404
Moon P and Koshino M 2013 *Phys. Rev.* B **88** 241412
[21] Le H A *et al* 2014 *J. Phys.: Condens. Matter* **26** 405304
[22] Yang K *et al* 2016 *Sci. Rep.* **6** 23897
[23] Morimoto T *et al* 2009 *Phys. Rev. Lett.* **103** 116803
Morimoto T *et al* 2012 *Phys. Rev.* B **86** 155426
[24] Crassee I *et al* 2011 *Nat. Phys.* **7** 48–51
[25] Falkovsky L A 2013 *JETP Lett.* **97** 429–38
[26] Shimano R *et al* 2013 *Nat. Commun.* **4** 1841
[27] Sounas D L *et al* 2013 *Appl. Phys. Lett.* **102** 191901
[28] Heyman J N *et al* 2014 *J. Appl. Phys.* **116** 214302
[29] Skulason H S *et al* 2015 *Appl. Phys. Lett.* **107** 093106
[30] Schiefele J *et al* 2016 *Phys. Rev.* B **94** 035401
[31] Kuzmin D A *et al* 2016 *Nano Lett.* **16** 4391–5
[32] Pereira V M *et al* 2010 *Europhys. Lett.* **92** 67001
[33] Pellegrino F M D *et al* 2010 *Phys. Rev.* B **81** 035411
[34] Dong B *et al* 2014 *Nanotechnology* **25** 455707
[35] Ni G-X *et al* 2014 *Adv. Mater.* **26** 1081–6
[36] Oliva-Leyva M and Naumis G G 2016 *Phys. Rev.* B **93** 035439
Oliva-Leyva M and Naumis G G 2015 *2D Mater.* **2** 025001
[37] Soler J M *et al* 2002 *J. Phys.: Condens. Matter* **14** 2745
[38] Lherbier A *et al* 2012 *Phys. Rev.* B **86** 075402
[39] Pereira V M *et al* 2009 *Phys. Rev.* B **80** 045401
[40] Santoso I *et al* 2014 *Phys. Rev.* B **89** 075134
Majidi M A *et al* 2014 *Phys. Rev.* B **90** 195442
Gogoi P K *et al* 2015 *Phys. Rev.* B **91** 035424
[41] Guinea F *et al* 2010 *Nat. Phys.* **6** 30–3
[42] Blakslee O L *et al* 1970 *J. Appl. Phys.* **41** 3373
[43] Lherbier A *et al* 2016 *2D Mater.* **3** 045006